SIMPLE SPECTRAL GRAPH CONVOLUTION

Anonymous authors
Paper under double-blind review

ABSTRACT

Graph Convolutional Networks (GCNs) have drawn significant attention and become leading methods for learning graph representations. The most GCNs suffer the performance loss when the depth of the model increases. Similarly to CNNs, without specially designed architectures, the performance of a network degrades quickly with increased depth. Some researchers argue that the required neighbourhood size and neural network depth are two completely orthogonal aspects of graph representation. Thus, several methods extend the neighbourhood by aggregating k-hop neighbourhoods of nodes while using shallow neural networks. However, these methods still encounter oversmoothing, high computation and storage costs. In this paper, we use the Markov Diffusion Kernel to derive a variant of GCN called Simple Spectral Graph Convolution (S^2GC) which is closely related to spectral models and combines strengths of both spatial and spectral methods. Our spectral analysis shows that our simple spectral graph convolution used in S^2GC is a trade-off of low-pass and high-pass filter which captures the global and local contexts of each node. Our experimental evaluation demonstrates that S^2GC with a linear learner is competitive in text, node and graph classification tasks. Moreover, S^2GC is comparable to other state-of-the-art methods for node clustering and community prediction tasks.

1 INTRODUCTION

In the past few years, the rise and application of deep learning have successfully promoted the research of computer vision and data mining. Although these deep learning methods have been applied to extract the features on the Euclidean lattice (spatial data) with great success, the data in many practical scenarios lies on non-Euclidean structures. Processing non-Euclidean structures is a challenge for deep learning methods. By defining a convolution operator between the graph and signal, Graph Convolutional Networks (GCNs) generalize Convolutional Neural Networks (CNNs) to graph-structured inputs which contain attributes. Message Passing Neural Networks (MPNNs) (Gilmer et al., 2017) unify the graph convolution as two functions: the transformation function and the aggregation function. MPNN iteratively propagates node features based on the adjacency structure of graph in a number of rounds.

Despite their enormous success in many applications like social media, traffic analysis, biology, recommendation systems and even computer vision, most of the current GCN models use shallow architectures because many of the recent models such as GCN (Kipf & Welling, 2016) achieve their best performance with 2-layer models. In other words, 2-layer GCN models aggregate nodes in two-hops neighbourhood and thus have no ability to extract information in k-hops neighbourhoods for $k > 2$. Moreover, stacking more layers and adding a non-linearity tends to degrade the performance of these models. Such a phenomenon is called oversmoothing (Li et al., 2018a), which suggests that as the number of layers increases, the representations of the nodes in GCNs are inclined to converge to a certain value and become less distinct from one another. Even adding residual connections, an effective trick for training very deep neural networks in computer vision, merely slows down the oversmoothing issue (Kipf & Welling, 2016) in GCNs. It appears that deep GCN models gain nothing but the performance degradation from the deep architecture.

One solution for that is only widening the aggregation function but keeping the same transformation function because the required neighbourhood size and neural network depth can be regarded as two orthogonal aspects of design. SGC (Wu et al., 2019) attempts to capture the context from K-hops neighbours in the graph by applying the K-th power of the graph convolution matrix in a single

neural network layer. This scheme is also used for attributed graph clustering (Zhang et al., 2019). However, SGC is also suffering from oversmoothing as $K \to \infty$ as shown in Theorem 1. PPNP and APPNP (Klicpera et al., 2019a) replace the power of the graph convolution matrix with the Personalized PageRank matrix to solve the oversmoothing problem. Although APPNP relieve the oversmoothing problem, it employs a non-linear operation which requires costly computation of the derivative of the filter due to the non-linearity over the multiplication of feature matrix with learnable weights. In contrast, we show that our approach enjoys a free derivative computed in the feed-forward step thanks to the use of linear model. Furthermore, APPNP aggregates over multiple k-hop neighborhoods but the weighting scheme favors either global or local context making it difficult if not impossible to find the balancing parameter. In contrast, our approach does aggregate over k-hop neighborhoods in a balanced manner as shown later in the text.

GDC (Klicpera et al., 2019b) further extends APPNP by generalizing Personalized PageRank (Page et al., 1999) to an arbitrary graph diffusion process. GDC, technically, has stronger expressive power than SGC (Wu et al., 2019), PPNP and APPNP (Klicpera et al., 2019a) but it leads to a dense transition matrix which makes the computation and space storage intractable for large graphs although authors suggest that the shrinkage method can be used to sparsify the generated transition matrix by ignoring small values.

To solve the above issues, we propose a Simple Spectral Graph Convolution (S^2GC) network for node clustering (semi-supervised and unsupervised setting), node classification and graph classification. By analyzing Markov Diffusion Kernel (Fouss et al., 2012), we obtain a very simple and effective filter: we aggregate k-step diffusion matrices over $k = 0, \cdots, K$ steps which is equivalent to aggregating over neighborhoods of various sizes. Moreover, we show that our design incorporates larger neighborhoods compared to SGC thus coping better with oversmoothing. We explain that limiting over-dominance of the largest neighborhoods in the aggregation step is a desired approach to limit oversmoothing while preserving large context of each node. We also show that in spectral analysis that S^2GC is a trade-off between the low- and high-pass filters which leads to capturing the global and local contexts of each node. Moreover, we show how S^2GC and APPNP (Klicpera et al., 2019a) are related and explain why S^2GC captures a range of neighborhoods better than APPNP. Our experimental results include node clustering, unsupervised and semi-supervised node classification, node property prediction and supervised text classification. We show that S^2GC is highly competitive often significantly outperforming state-of-the-art methods.

2 Preliminaries

Notations. Let $G = (V, E)$ be a simple and connected undirected graph with n nodes and m edges. We use $\{1, \cdots, n\}$ to denote the node index of G, and d_j denote the degree of node j in G. Let $\mathbf{A}$ be the adjacency matrix and $\mathbf{D}$ the diagonal degree matrix. Let $\widetilde{\mathbf{A}} = \mathbf{A} + \mathbf{I}_n$ denote the adjacency matrix with added self-loops and the corresponding diagonal degree matrix $\widetilde{\mathbf{D}}$ where $\mathbf{I}_n \in \mathcal{S}_{++}^n$ is an identity matrix. Finally, let $\mathbf{X} \in \mathbb{R}^{n \times d}$ denote the node feature matrix and each node v is associated with a d-dimensional feature vector $\mathbf{X}_v$. The normalized graph Laplacian matrix is defined as $\mathbf{L} = \mathbf{I}_n - \mathbf{D}^{-1/2}\mathbf{A}\mathbf{D}^{-1/2} \in \mathcal{S}_{+}^n$, a symmetric positive semidefinite matrix with eigendecomposition $\mathbf{U}\mathbf{\Lambda}\mathbf{U}^\top$. Here $\mathbf{\Lambda}$ is a diagonal matrix of the eigenvalues of $\mathbf{L}$, and $\mathbf{U} \in \mathbb{R}^{n \times n}$ is a unitary matrix that consists of the eigenvectors of $\mathbf{L}$.

Spectral Graph Convolution (Defferrard et al., 2016). We consider spectral convolutions on graphs defined as the multiplication of a signal $\mathbf{x} \in \mathbb{R}^n$ with a filter g_θ parameterized by $\boldsymbol{\theta} \in \mathbb{R}^n$ in the Fourier domain:

$$g_\theta(\mathbf{L}) * x = \mathbf{U} g_\theta^*(\mathbf{\Lambda}) \mathbf{U}^\top \mathbf{x}, \tag{1}$$

where the parameter $\boldsymbol{\theta} \in \mathbb{R}^n$ is a vector of spectral filter coefficients. We can understand g_θ as a function operating on eigenvalues of $\mathbf{L}$, that is $g_\theta^*(\mathbf{\Lambda})$. To avoid eigendecomposition, $g_\theta(\mathbf{\Lambda})$ can be approximated by a truncated expansion in terms of Chebyshev polynomials $T_k(\mathbf{\Lambda})$ up to the K-th order (Defferrard et al., 2016):

$$g_\theta^*(\mathbf{\Lambda}) \approx \sum_{k=0}^{K-1} \theta_k T_k(\tilde{\mathbf{\Lambda}}), \tag{2}$$

with a rescaled $\tilde{\mathbf{\Lambda}} = \frac{1}{2\lambda_{\max}}\mathbf{\Lambda} - \mathbf{I}_n$ where $\lambda_{\max}$ denotes the largest eigenvalue of $\mathbf{L}$ and $\boldsymbol{\theta} \in \mathbb{R}^K$ is now a vector of Chebyshev coefficients.

Vanila Graph Convolutional Network (GCN) (Kipf & Welling, 2016). The vanilla GCN is a first-order approximation of spectral graph convolutions. If one sets $K = 1$, $\theta_0 = 2$, and $\theta_1 = -1$ for Eq. 2 they obtain the convolution operation $g_\theta(\mathbf{L}) * \mathbf{x} = (\mathbf{I} + \mathbf{D}^{-1/2}\mathbf{A}\mathbf{D}^{-1/2})\mathbf{x}$. Finally, by the renormalization trick, replacing the matrix $\mathbf{I} + \mathbf{D}^{-1/2}\mathbf{A}\mathbf{D}^{-1/2}$ by a normalized version $\widetilde{\mathbf{T}} = \widetilde{\mathbf{D}}^{-1/2}\widetilde{\mathbf{A}}\widetilde{\mathbf{D}}^{-1/2} = (\mathbf{D} + \mathbf{I}_n)^{-1/2}(\mathbf{A} + \mathbf{I}_n)(\mathbf{D} + \mathbf{I}_n)^{-1/2}$ leads to the GCN layer with σ, a non-linear function, *e.g.* ReLU:

$$H^{(l+1)} = \sigma(\widetilde{\mathbf{T}}\mathbf{H}^{(l)}\mathbf{W}^{(l)}), \tag{3}$$

Graph Diffusion Convolution (GDC) (Klicpera et al., 2019b). A generalized graph diffusion is given by the diffusion matrix:

$$\mathbf{S} = \sum_{k=0}^{\infty} \theta_k \mathbf{T}^k, \tag{4}$$

with the weighting coefficients θ_k and the generalized transition matrix $\mathbf{T}$. Eq. 4 can be regarded as related to the Taylor expansion of matrix-valued functions. Thus, the choice of θ_k and $\mathbf{T}^k$ must at least ensure that Eq. 4 converges. Klicpera et al. (2019b) provide two special cases as low-pass filters, *ie*. heat kernel and the kernel based on random walk with restarts. If $\mathbf{S}$ denote the adjacency matrix and $\mathbf{D}$ be the diagonal degree matrix of $\mathbf{S}$ then the corresponding graph diffusion convolution is defined as $\mathbf{D}^{-1/2}\mathbf{S}\mathbf{D}^{-1/2}\mathbf{x}$. Note that θ_k can be a learnable parameter, or it can be chosen in one or another way. Many works use expansion in Eq. 4 but different choices of θ_k realise very different filters making each method unique. One example may be Chebynet (Zhang et al., 2019).

Simple Graph Convolution (SGC) (Wu et al., 2019). A classical MPNN (Gilmer et al., 2017) averages in each layer the hidden representations among 1-hop neighbors. This implies that each node in the k-th layer obtains feature information from all nodes that are k-hops away in the graph. By hypothesizing that the non-linearity between GCN layers is not critical, SGC captures information from k-hops neighbourhood in the graph by applying the K-th power of the transition matrix in a single neural network layer. The SGC can be regarded as a special case of GDC without non-linearity and without the normalization by $\mathbf{D}^{-1/2}$ if we set $\theta_k = 1$ and $\theta_{i<K} = 0$ for Eq. 5, and $\mathbf{T} = \widetilde{\mathbf{T}}$:

$$\hat{Y} = \text{softmax}(\widetilde{\mathbf{T}}^K\mathbf{X}\mathbf{W}). \tag{5}$$

Although SGC is an efficient and effective method, increasing Kleads to oversmoothing. Thus, SGC uses similar K number of layers as GCN. We provide Theorem 1 to demonstrate that oversmoothing is a result of convergence to the stationary distribution in graph diffusion as time $t \to \infty$.

Theorem 1. *(Chung & Graham, 1997) Let λ_2 denote second largest eigenvalue of transition matrix $\widetilde{\mathbf{T}} = \mathbf{D}^{-1}\mathbf{A}$ of a non-bipartite graph, $\mathbf{p}(t)$ be the probability distribution vector and $\boldsymbol{\pi}$ the stationary distribution. If walk starts from the vertex i , $p_i(0) = 1$, then after t steps for every vertex:*

$$|p_j(t) - \pi_j| \leq \sqrt{\frac{d_j}{d_i}}\lambda_2^t, \tag{6}$$

APPNP. Klicpera et al. (2019a) proposed APPNP which uses Personalized PageRank to derive a fixed filter of order K. Let $f_\theta(\mathbf{X})$ denote the output of a two-layer fully connected neural network on the feature matrix $\mathbf{X}$, the PPNP model is defined as $\mathbf{H} = \alpha\mathbf{I}_n - (1-\alpha)\widetilde{\mathbf{T}}^{-1}f_\theta(\mathbf{X})$. To avoid calculating the inverse of matrix $\widetilde{\mathbf{T}}$, Klicpera et al. (2019a) also proposes Approximate PPNP (APPNP) which replaces the costly inverse with an approximation derived by the truncated power iteration:

$$\mathbf{H}^{(l+1)} = (1-\alpha)\widetilde{\mathbf{T}}\mathbf{H}^{(l)} + \alpha\mathbf{H}^{(0)}, \tag{7}$$

where $\mathbf{H}^{(0)} = f_\theta(\mathbf{X}) = \text{ReLU}(\mathbf{X}\mathbf{W})$. By decoupling the feature transformation and propagation steps, PPNP and APPNP aggregate information from multi-hop neighbors.

3 METHODOLOGY

In this section, firstly we briefly discuss the spectral analysis and graph partitioning, and conclude the small eigenvalues of a Laplacian matrix control global clustering which partitions the graph into a few of large clusters. Secondly, we analyze the Markov Diffusion Kernel (Fouss et al., 2012) and note that the corresponding feature mapping function acts as a low-pass filter. Finally, based on the feature mapping function we present our Simple Spectral Graph Convolution network.

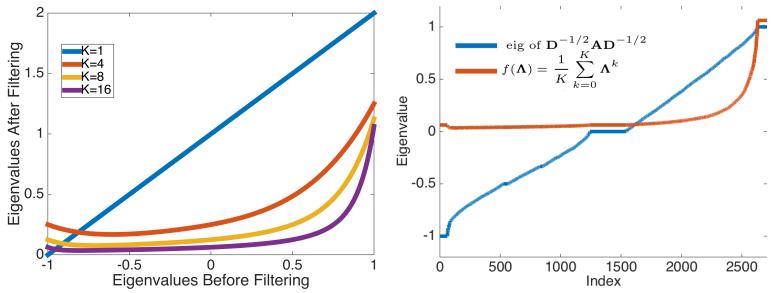

(a) (b)

Figure 1: (a) Function $f(\lambda) = \frac{1}{K}\sum_{k=0}^{K}\lambda^k$ with $\lambda \in [-1, 1]$, $K \in \{1, 4, 8, 16\}$; (b) Sorted by index, eigenvalues of $\mathbf{D}^{-1/2}\mathbf{A}\mathbf{D}^{-1/2}$ and push-forward eigenvalues $f(\mathbf{\Lambda}) = \frac{1}{K}\sum_{k=0}^{K}\mathbf{\Lambda}^k$ on Cora network ($K = 16$).

3.1 Spectral analysis and graph partitioning

Our design follows Claims I and II described in Section A.3.1 which includes their proofs.

Claim I. Our filter, by design, will give the highest weight to the closest neighborhood of a node as neighborhoods $\mathcal{N}$ of diffusion steps $k = 0, \cdots, K$ obey: $\mathcal{N}(\widetilde{\mathbf{T}}^0) \subseteq \mathcal{N}(\widetilde{\mathbf{T}}^1) \subseteq \cdots \subseteq \mathcal{N}(\widetilde{\mathbf{T}}^K) \subseteq \mathcal{N}(\widetilde{\mathbf{T}}^\infty)$. That is, smaller neighbourhoods belong to larger neighbourhoods too.

Claim II. As $K \to \infty$, the ratio of energies contributed by S^2GC to SGC is 0. Thus, the energy of infinite-dimensional receptive field (largest k) will not dominate the sum energy of our filter. Thus, S^2GC can incorporate larger receptive fields without overbearing contributions of smaller receptive fields. This is substantiated by Table 8 where we achieve $K = 16$ while SGC achieves $K = 4$.

3.2 Markov Diffusion Kernel

Two nodes are considered similar when they are diffused in a similar way through the graph, and therefore when they influence the other nodes in a similar manner (Fouss et al., 2012). In other words, two nodes are close if they are in the same cluster which has a consistent local structure. More precisely, the diffusion distance at time K between nodes i and j is defined as follows:

$$d_{ij}(K) = \|\mathbf{x}_i(K) - \mathbf{x}_j(K)\|_2^2, \tag{8}$$

where the average visiting rate $\mathbf{x}_i(K)$ after K steps for a process that started at time $k = 0$ is computed as follows:

$$\mathbf{x}_i(K) = \frac{1}{K}\sum_{k=1}^{K}\mathbf{T}^k\mathbf{x}_i(0). \tag{9}$$

By defining $\mathbf{Z}(K) = \frac{1}{K}\sum_{k=1}^{K}\mathbf{T}^k$, we reformulate Eq. 8 as a metric given as:

$$d_{ij}(K) = \|\mathbf{Z}(K)(\mathbf{x}_i(0) - \mathbf{x}_j(0))\|_2^2. \tag{10}$$

The underlying feature map of Markov Diffusion Kernel (MDK) is given as $\mathbf{Z}(K)\mathbf{x}_i(0)$ for node i.

The effect of the linear projection $\mathbf{Z}(K)$ (filter) acting on spectrum as $f(\lambda) = \frac{1}{K}\sum_{k=0}^{K}\lambda^k$ (we sum from 0 to include self-loops) is plotted in Figure 1, from which we observe the following properties: (i) $\mathbf{Z}(K)$ preserves leading (large) eigenvalues of $\mathbf{T}$ and (ii) the higher K is the stricter the low-pass filter becomes but the filter also preserves the high frequency. In other words, as K grows, this filter includes larger and larger neighborhood but also maintains the closest locality of nodes. Note that $\mathbf{L} = \mathbf{I} - \mathbf{T}$ where $\mathbf{L}$ is the normalized Laplacian matrix and $\mathbf{T}$ is the normalized adjacency matrix. Thus keeping large positive eigenvalues for $\mathbf{T}$ equals keeping small eigenvalues for $\mathbf{L}$.

3.3 SIMPLE SPECTRAL GRAPH CONVOLUTION

Based on the aforementioned Markov Diffusion Kernel, we include self-loops and we propose the Simple Spectral Graph Convolution (S^2GC) network with a softmax after a linear layer:

$$\hat{Y} = \text{softmax}(\frac{1}{K}\sum_{k=0}^{K}\widetilde{\mathbf{T}}^k\mathbf{X}\mathbf{W}). \tag{11}$$

As $K \to \infty$, $\mathbf{H} = \sum_{k=1}^{\infty}\widetilde{\mathbf{T}}^k$ is the optimal diffused representation of the normalized Laplacian Regularization problem (Chapelle et al., 2006):

$$\min_{\mathbf{H}} \frac{1}{2}\sum_{i,j=1}^{n}\widetilde{\mathbf{A}}_{ij}\|\frac{\mathbf{h}_i}{\sqrt{d_i}} - \frac{\mathbf{h}_j}{\sqrt{d_j}}\|_2^2 + \|\mathbf{h}_i - \mathbf{x}_i\|_2^2, \tag{12}$$

where each vector $\mathbf{h}_i$ denotes the i-th row of $\mathbf{H}$. However, the infinite expansion resulting from Eq. 12 in fact is suboptimal due to oversmoothing (Fig. 8 shows this). In contrast, we include in Eq. 11 a self-loop $\widetilde{T}^0 = \mathbf{I}$, the $\alpha \in [0, 1]$ parameter (Fig. 9 evaluates its impact) to balance the node's self information *vs*. consecutive neighborhoods, and we consider finite K. We generalize the Eq. 11 as:

$$\hat{Y} = \text{softmax}\left(\frac{1}{K}\sum_{k=1}^{K}\left((1-\alpha)\,\widetilde{\mathbf{T}}^k\mathbf{X} + \alpha\mathbf{X}\right)\mathbf{W}\right). \tag{13}$$

Relation of S^2GC to GDC. GDC uses the entire filter matrix $\mathbf{S}$ $(n \times n)$ as $\mathbf{S}$ is then re-normalized by its degree. Klicpera et al. (2019b) explain that 'Most graph diffusions result in a dense matrix $\mathbf{S}$.

In contrast, our approach is simply computed as $(\sum_{k=1}^{K}\widetilde{\mathbf{T}}^k\mathbf{X})\mathbf{W}$ (plus self-loop) where $\mathbf{X}$ is of size $(n \times d)$ where $d \ll n$, n and d being the number of nodes and features, respectively. The $\widetilde{\mathbf{T}}^\tau\mathbf{X}$ step is computed as $\widetilde{\mathbf{T}}\cdot(\widetilde{\mathbf{T}}\cdot(\cdots(\widetilde{\mathbf{T}}\mathbf{X})\cdots))$ which requires t matrix-matrix multiplications between matrices of size $n \times n$ and $n \times d$. Thus, S^2GC can handle extremely large graphs as it does not need to sparsify dense filter matrices as GDC.

Relation of S^2GC to APPNP. Let us define $\mathbf{H}^0 = \mathbf{X}\mathbf{W}$ as we use the linear step in our S^2GC. Then and only then, for $l = 0$ and $\mathbf{H}^0 = \mathbf{X}\mathbf{W}$, APPNP expansion yields $\mathbf{H}^1 = (1-\alpha)\widetilde{\mathbf{T}}\mathbf{X}\mathbf{W} + \alpha\mathbf{X}\mathbf{W} = ((1-\alpha)\widetilde{\mathbf{T}} + \alpha\mathbf{I})\mathbf{X}\mathbf{W}$ which is equal to our $\mathbf{Z}(1)\mathbf{X}\mathbf{W} = (\sum_{k=0}^{K}\widetilde{\mathbf{T}}^k)\mathbf{X}\mathbf{W} = \widetilde{\mathbf{T}}\mathbf{X} + \mathbf{X} = (\widetilde{\mathbf{T}} + \mathbf{I})\mathbf{X}\mathbf{W}$ if $\alpha = 0.5$, $K = 1$, except for scaling (constant) of $\mathbf{H}^1$.

In contrast, for $l = 1$ and general case $\mathbf{H}^0 = f(\mathbf{X};\mathbf{W})$, APPNP yields $\mathbf{H}^2 = (1-\alpha)^2\widetilde{\mathbf{T}}^2 f(\mathbf{X};\mathbf{W}) + (1-\alpha)\alpha\widetilde{\mathbf{T}}f(\mathbf{X};\mathbf{W}) + \alpha f(\mathbf{X};\mathbf{W})$ from which is is easy to note specific weight coefficients $(1-\alpha)^2$, $(1-\alpha)\alpha$ and α associated with 2-, 1-, and 0-hops. This shows that the APPNP expansion is very different to S^2GC expansion in Eq. 13. In fact, S^2G and APPNP are only equivalent if $\alpha = 0.5$, $K = 1$ and a linear transformation f is used.

Moreover, APPNP assumes $\mathbf{H}^0 = f(\mathbf{X};\mathbf{W}) = \text{ReLU}(\mathbf{X}\mathbf{W})$, thus their optimizer has to back-propagate through $f(\mathbf{X};\mathbf{W})$ to obtain $\frac{\partial f}{\partial \mathbf{W}}$ and multiply this with the above expansion *e.g.*, $\frac{\partial \mathbf{H}^2}{\partial \mathbf{W}} = (1-\alpha)^2\widetilde{\mathbf{T}}^2 f'(\mathbf{X};\mathbf{W}) + (1-\alpha)\alpha\widetilde{\mathbf{T}}f'(\mathbf{X};\mathbf{W}) + \alpha f'(\mathbf{X};\mathbf{W})$.

In contrast, we use the linear function $\mathbf{X}\mathbf{W}$. Thus, $\frac{\partial \mathbf{X}\mathbf{W}}{\partial \mathbf{W}}$ yields $\mathbf{X}$. Thus, the multiplication of our expansion with $\mathbf{X}$ for the backprop step is in fact obtained in the forward pass which makes our approx very fast for large graphs.

Relation of S^2GC to AR. The AR filter (Li et al., 2019) uses the regularized Laplacian kernel (Smola & Kondor, 2003) which differs from used by us (modified) Markov diffusion kernel. Specifically, the regularized Laplacian kernel uses the negated Laplacian matrix yielding $-\mathbf{L}$ as follows: $\mathbf{K}_{\text{L}} = \sum_{k=0}^{\infty}\alpha^k(-\mathbf{L})^k = (\mathbf{I} + \alpha\mathbf{L})^{-1}$ where $\mathbf{L} = \mathbf{I} - \widetilde{\mathbf{T}}$ which is related to the von Neumann diffusion kernel $\mathbf{K}_{\text{vN}} = \sum_{k=0}^{\infty}\alpha^k\mathbf{A}^k$. In contrast, the Markov diffusion kernel $\mathbf{K}_{\text{MD}}(K) = \mathbf{Z}(K)\mathbf{Z}^{\text{T}}(K)$ where $\mathbf{Z}(K) = \frac{1}{K}\sum_{k=1}^{K}\widetilde{\mathbf{T}}^k$, where $\widetilde{\mathbf{T}} = \mathbf{D}^{-1/2}\mathbf{A}\mathbf{D}^{-1/2}$.

Table 1: Computational and storage complexities $\mathcal{O}(\cdot)$.

Stage	Complexity	APPNP	GDC	SGC	S^2GC
Forward Propagation	Computation Cost	$K\|E\|d + Knd$	$\approx K\|E\|n$	$K\|E\|d$	$K\|E\|d + Knd$
	Storage Cost	$nd + \|E\|$	$\approx n^2$	$nd + \|E\|$	$nd + \|E\|$
Backward Propagation	Computation Cost	$K\|E\|d$	0	0	0
	Storage Cost	$nd + \|E\|$	0	0	0

Table 2: Timing (seconds) on Cora, Citeseer, Pubmed and the large scale Open Graph Benchmark (OGB) which includes Products.

methods	Cora	Citeseer	Pubmed	Products
SGC	0.45	0.55	0.78	9.8
APPNP	1.08	1.44	1.32	748
S^2GC	0.67	0.81	0.79	11.4

Relation of S^2GC to Jumping Knowledge Network (JKN). Xu et al. (2018b) combine intermediate node representations from each layer by concatenating them in the final layer. However, (Xu et al., 2018b) use non-linear layers which results in a completely different network architecture and the usual slower processing due to complex backpropagation chain.

3.4 Complexity Analysis

For S^2GC, the storage costs is $\mathcal{O}(|E| + nd)$, where $|E|$ is the total edge count, nd relates to saving the $\widetilde{\mathbf{T}}^k\mathbf{X}$ during intermediate multiplications $\widetilde{\mathbf{T}} \cdot (\widetilde{\mathbf{T}} \cdot (\cdots (\widetilde{\mathbf{T}}\mathbf{X}) \cdots))$. The computational cost is the $\mathcal{O}(K|E|d + Knd)$. Each sparse matrix multiplication $\widetilde{\mathbf{T}}\mathbf{X}$ costs $|E|d$ and we need K such multiplications while Knd realises summation over filters and nd is the cost of adding features $\mathbf{X}$.

In contrast, the storage cost of GDC is approximately $\mathcal{O}(n^2)$ and the computational cost is approximately $\mathcal{O}(K|E|n)$ where n is the node numbers, K is the order of terms and $|E|$ is the number of graph edges. APPNP, SGC and S^2GC have much lower cost than GDC. Kindly note $K|E|d \gg Knd$ and $n \gg d$. We found that APPNP, SGC and S^2GC have similar computational and storage costs in the forward stage. Note that the d in APPNP is not the dimension of features $\mathbf{X}$ but $f(\mathbf{X})$, which is the number of categories.

For the backward stage including computing the gradient of the classification step, the computational costs of GDC, SGC and S^2GC are independent of K and $|E|$ because the graph convolution for these methods does not require backprop (grad. is computed in the forward step). In contrast, APPNP requires backprop as explained earlier.

Table 1 summarizes the computational and storage costs of several methods. Table 2 demonstrates that APPNP is over 66$\times$ slower than S^2GC on large scale Products dataset (OGB benchmark) despite, for fairness, we use the same basic building blocks of PyTorch among compared methods.

4 Experiments

In this section, we evaluate the proposed method on four different tasks: node clustering, community prediction, semi-supervised node classification and text classification.

4.1 Node Clustering

We compare S^2GC with three kinds of clustering methods: (i) Methods that only use node features: k-means and spectral clustering (spectral-f) that constructs a similarity matrix with the node features by a linear kernel. (ii) Structural clustering methods that only use graph structures: spectral clustering (spectral-g) that takes the node adjacency matrix as the similarity matrix, DeepWalk (Perozzi et al., 2014), and (iii) Attributed graph clustering methods that utilize both node features and graph structures: Graph Autoencoder (GAE) and Graph Variational Autoencoder (VGAE) (Kipf & Welling, 2016), and Adversarially Regularized Graph Autoencoder (ARGE), Variational Graph

Table 3: Clustering performance with three different metrics on four datasets.

Methods	Input	Cora			Citeseer			Pubmed			Wiki		
		Acc%	NMI%	F1%	Acc%	NMI%	F1%	Acc%	NMI%	F1%	Acc%	NMI%	F1%
k-means	Feature	34.65	16.73	25.42	38.49	17.02	30.47	57.32	29.12	57.35	33.37	30.20	24.51
Spectral-f	Feature	36.26	15.09	25.64	46.23	21.19	33.70	59.91	32.55	58.61	41.28	43.99	25.20
Spectral-g	Graph	34.19	19.49	30.17	25.91	11.84	29.48	39.74	3.46	51.97	23.58	19.28	17.21
DeepWalk	Graph	46.74	31.75	38.06	36.15	9.66	26.70	61.86	16.71	47.06	38.46	32.38	25.74
GAE	Both	53.25	40.69	41.97	41.26	18.34	29.13	64.08	22.97	49.26	17.33	11.93	15.35
VGAE	Both	55.95	38.45	41.50	44.38	22.71	31.88	65.48	25.09	50.95	28.67	30.28	20.49
ARGE	Both	64.00	44.90	61.90	57.30	35.00	54.60	59.12	23.17	58.41	41.40	39.50	38.27
ARVGE	Both	62.66	45.28	62.15	54.40	26.10	52.90	58.22	20.62	23.04	41.55	40.01	37.80
AGC	Both	68.92	53.68	65.61	67.00	41.13	62.48	69.78	31.59	68.72	47.65	45.28	40.36
S^2GC	Both	**69.60**	**54.71**	**65.83**	**69.11**	**42.87**	**64.65**	**70.98**	**33.21**	**70.28**	**52.67**	**49.62**	**44.31**

Autoencoder (ARVGE) (Pan et al., 2018) and AGC (Zhang et al., 2019). To evaluate the clustering performance, three performance measures are adopted: clustering Accuracy (Acc), Normalized Mutual Information (NMI) and macro F1-score (F1). We run each method 10 times on four datasets: Cora, CiteSeer, PubMed, and Wiki, and we report the average clustering results in Table 3, where top-1 results are highlighted in bold. To adaptively select the order k, we use the clustering performance metric: internal criteria based on the information intrinsic to the data alone Zhang et al. (2019).

4.2 Community Prediction

We supplement our social network analysis by using S^2GC to inductively predict the community structure on Reddit, a large scale dataset as shown in Table 11 which cannot be processed by the vanilla GCN Kipf & Welling (2016) and GDC (Klicpera et al., 2019b) due to the memory issues. On the Reddit dataset, we train S^2GC with L-BFGS using no regularization, and we set $K = 5$ and $\alpha = 0.05$. We evaluate S^2GC inductively according to protocol (Chen et al., 2018). We train S^2GC on a subgraph comprising only training nodes and test on the original graph. On all datasets, we tune the number of epochs based on both convergence behavior and the obtained validation accuracy.

For Reddit, we compare S^2GC to the reported performance of supervised and unsupervised variants of GraphSAGE (Hamilton et al., 2017), FastGCN (Chen et al., 2018), SGC (Wu et al., 2019) and DGI (Velickovic et al., 2019). Table 4 also highlights the setting of the feature extraction step for each method. Note that S^2GC and SGC involve no learning because they do not learn any parameters to extract features. The logistic regression is used as a classifier for both unsupervised and no-learning approaches to train with labels afterward.

4.3 Node Classification

For the semi-supervised node classification task, we apply the standard fixed training/validation/testing split (Yang et al., 2016) on the Cora, Citeseer, and Pubmed datasets, with 20 nodes per class for training, 500 nodes for validation and 1,000 nodes for testing. For baselines, We include three state-of-the-art shallow models: GCN (Kipf & Welling, 2016), GAT (Veličković et al., 2017), FastGCN (Chen et al., 2018), APPNP (Klicpera et al., 2019a), Mixhop (Abu-El-Haija et al., 2019), SGC (Wu et al., 2019), DGI (Velickovic et al., 2019) and GIN (Xu et al., 2018a). We use the Adam SGD optimizer (Kingma & Ba, 2014) with a learning rate of 0.02 to train S^2GC. We set $\alpha = 0.05$ and $K = 16$ on all datasets. We perform a grid search to tune the weight decay for models with different depths based on the accuracy and loss of the validation set. We will discuss the influences of α and K later.

To evaluate the proposed method on large scale benchmarks, we use ogbn-arxiv, ogbn-mag and ogbn-products to demonstrate the comparison among the proposed method, SGC, GraphSage, GCN, MLP and Softmax (multinomial Regression), as shown in Table 6. In these three datasets, our method outperforms SGC consistently. In ogbn-arxiv and ogbn-products, we can observe our method cannot outperforms GCN and GraphSage while MLP outperforms softmax classifier significantly. Thus we argue in these two datasets, MLP plays a more important role than graph convolution. To prove this point, we also conduct the experiment (S^2GC+MLP) that we use MLP to replace the linear classifier and obtain a more powerful S^2GC. In ogbn-mag, MLP barely helps our method because the performance of MLP is close to the one of Softmax. In other two datasets, the

Table 4: Test Micro F1 Score (%) averaged over 10 runs on Reddit. Performance of other models are cited from their original papers.

Setting	Model	Test F1
Supervised	SAGE-mean	95.0
	SAGE-LSTM	**95.4**
Unsupervised	SAGE-GCN	93.0
	FastGCN	93.7
No Learning	SAGE-GCN	90.8
	DGI	94.0±0.001
	SGC	94.9±0.001
	S^2GC	**95.3±0.001**

Table 5: Test accuracy (%) averaged over 10 runs on citation networks.

methods	Cora	Citeseer	Pubmed
GCN	81.4± 0.4	70.9± 0.5	79.0± 0.4
GAT	83.3± 0.7	72.6± 0.6	78.5± 0.3
FastGCN	79.8± 0.3	68.8± 0.6	77.4± 0.3
GIN	77.6± 1.1	66.1± 0.9	77.0± 1.2
DGI	82.5± 0.7	71.6± 0.7	78.4± 0.7
SGC	81.0± 0.02	71.9± 0.08	78.9± 0.03
MixHop	81.8±0.6	71.4±0.8	80.0±1.1
APPNP	**83.3±0.5**	71.7±0.6	80.1±0.2
Chebynet	78.0± 0.4	70.1± 0.5	78.0± 0.4
AR filter	80.8± 0.02	69.3± 0.15	78.1± 0.01
Ours	83.0± 0.02	**73.6± 0.09**	**80.4± 0.02**

Table 6: Test accuracy (%) averaged over 10 runs on OGB node property prediction .

methods	Products	Mag	Arxiv
MLP	61.06±0.08	26.92±0.26	55.50±0.23
GCN	75.64±0.21	30.43±0.25	71.74±0.29
GraphSage	**78.29±0.16**	31.53±0.15	71.49±0.27
Softmax	47.70±0.03	24.13±0.03	52.77±0.56
SGC	68.87± 0.01	29.47±0.03	68.78±0.02
S^2GC	70.22± 0.01	32.47±0.11	70.15±0.13
S^2GC+MLP	74.84±0.20	**32.72±0.23**	**72.01±0.25**

significant improvements are easy to observe that S^2GC with MLP is more close to GCN and even outperform it.

4.4 Text Classification

Text classification predicts the labels of documents. Yao et al. (2019) use a 2-layer GCN to achieve state-of-the-art results by creating a corpus-level graph which treats both documents and words as nodes in a graph. Word-to-word edge weights are given by Point-wise Mutual Information (PMI) and word-document edge weights are given by normalized TF-IDF scores.

We ran our experiments on five widely used benchmark corpora including movie review (MR), 20-Newsgroups (20NG), Ohsumed, R52 and R8 of Reuters 21578. We first preprocessed all the datasets by cleaning and tokenizing text as (Kim, 2014). We then removed stop words defined in NLTK6 and low frequency words appearing less than 5 times for 20NG, R8, R52 and Ohsumed. We compare two state-of-the-art models with our method: GCN (Kipf & Welling, 2016) and SGC (Wu et al., 2019). The statistics of the preprocessed datasets are summarized in Table 12. Table 7 shows that an S^2GC rivals their models on 5 benchmark datasets. We give the parameters setting in the supplementary material.

4.5 A detailed comparison with various numbers of layers and α

Table 8 summaries the results for the deep models with various numbers of layers (or K for SGC and our methods). We observe that on Cora, Citeseer and Pubmed that our method consistently obtains the best performance with $K = 16$ equivalent of 16 layers. Overall, the results suggest that with S^2GC, we can aggregate over larger neighborhood than SGC thus we suffer less from

Table 7: Test accuracy on the document classification task.

Model	**20NG**	**R8**	**R52**	**Ohsumed**	**MR**
Text GCN	87.9 ± 0.2	97.0 ± 0.2	93.8 ± 0.2	68.2 ± 0.4	76.3 ± 0.3
SGC	88.5 ± 0.1	97.2 ± 0.2	94.0 ± 0.2	**68.5 ± 0.3**	75.9 ± 0.3
S^2GC	**88.6± 0.1**	**97.4 ± 0.1**	**94.5 ± 0.2**	**68.5 ± 0.1**	**76.7 ± 0.0**

Table 8: Summary of classification accuracy (%) results with various depths. In the linear model, filter parameter K is equivalent with the number of layers.

Dataset	Method	Layers (K)					
		2	4	8	16	32	64
Cora	GCN	81.1	80.4	69.5	64.9	60.3	28.7
	SGC	80.8	81.5	80.7	79.0	75.9	66.8
	S^2GC	76.5	79.8	82.5	**83.0**	82.2	80.0
Citeseer	GCN	70.8	67.6	30.2	18.3	25.0	20.0
	SGC	71.9	72.6	73.1	72.2	70.6	69.2
	S^2GC	70.9	72.7	72.7	**73.4**	73.1	73.2
Pubmed	GCN	79.0	76.5	61.2	40.9	22.4	35.3
	SGC	79.2	79.7	78.4	76.4	71.6	68.6
	S^2GC	77.6	78.7	79.4	**80.6**	78.0	74.9

Table 9: Classification accuracy (%) results with different α.

Dataset	0.0	0.05	0.1	0.15
cora	82.9	83.0	82.6	81.9
citeseer	73	73.4	73.3	72.9
pubmed	80.4	80.6	79.7	79.0

oversmoothing. On the other hand, the performance of GCN and SGC drops rapidly as the number of layers exceeds 32 due to oversmoothing.

Table 9 summaries the results for the proposed method for various α ranged from 0 to 0.15. As we can observe, α only slightly improves the performance of S^2GC. Thus. balancing self-loop by α with other filters of consecutively larger receptive fields is useful but the self-loop is not mandatory.

Table 10: Graph Classification

Method	MUTAG	PROTEINS	COLLAB	IMDB- BINARY
GCN	74.6 ± 7.7	73.1 ± 3.8	80.6 ± 2.1	72.6 ± 4.5
SAGE	74.9 ± 8.7	73.8 ± 3.6	79.7 ± 1.7	72.4 ± 3.6
GIN-0	85.7 ± 7.7	72.1 ± 5.1	79.3 ± 2.7	72.8 ± 4.5
GIN-ϵ	83.4 ± 7.5	72.6 ± 4.9	79.8 ± 2.4	72.1 ± 5.1
DiffPool	85.0 ± 10.3	75.1 ± 3.5	78.9 ± 2.3	72.6 ± 3.9
S^2GC	85.1 ± 7.4	75.5 ± 4.1	80.2 ± 1.3	72.9 ± 4.9

4.6 Graph Classification

We report the average accuracy of 10-fold cross validation on a number of common benchmark datasets (as shown in Table 10), where we randomly sample a training fold to serve as a validation set. We only make use of discrete node features. In case they are not given, we use one-hot encodings of node degrees as feature input. We note that graph classification is a task highly dependent on the global pooling strategy. There exist methods that apply sophisticated mechanisms for this step. However, with a simple average pooling and a highly scalable S^2GC model, we comfortably outperform all methods on MUTAG, Proteins and IMDB-Binary.

5 Conclusions

We have proposed Simple Spectral Graph Convolution (S^2GC), a method based on the Markov Diffusion Kernel (Section 3.2) whose feature maps emerge from the normalized Laplacian Regularization problem (Section 3.3). The theoretical analysis shows that S^2GC benefits from the right level of trade-off in the aggregation over consecutively larger receptive fields. We have shown there exist a connection between S^2GC and other methods such as SGC, APPNP and JKN by analyzing spectral properties and implementation of each model. However, ac our Claims I and II show, we have designed a filter with unique properties to capture larger context while limiting oversmoothing. S^2GC inherits many of the strengths of spectral methods and none of their weaknesses, *e.g.* oversmoothing. We have conducted extensive and rigorous experiments that have shown that S^2GC is competitive and frequently outperforms many state-of-the-art methods on unsupervised, semi-supervised and supervised tasks and several popular datasets.

REFERENCES

Sami Abu-El-Haija, Bryan Perozzi, Amol Kapoor, Nazanin Alipourfard, Kristina Lerman, Hrayr Harutyunyan, Greg Ver Steeg, and Aram Galstyan. Mixhop: Higher-order graph convolutional architectures via sparsified neighborhood mixing. In *International Conference on Machine Learning*, pp. 21–29, 2019.

Afonso S Bandeira, Amit Singer, and Daniel A Spielman. A cheeger inequality for the graph connection laplacian. *SIAM Journal on Matrix Analysis and Applications*, 34(4):1611–1630, 2013.

Olivier Chapelle, Bernhard Schölkopf, and Alexander Zien. Semi-supervised learning (adaptive computation and machine learning), 2006.

Jie Chen, Tengfei Ma, and Cao Xiao. Fastgcn: Fast learning with graph convolutional networks via importance sampling. In *International Conference on Learning Representations*, 2018.

Fan RK Chung and Fan Chung Graham. *Spectral graph theory*. Number 92. American Mathematical Soc., 1997.

Kenneth Ward Church and Patrick Hanks. Word association norms, mutual information, and lexicography. *Computational linguistics*, 16(1):22–29, 1990.

Michaël Defferrard, Xavier Bresson, and Pierre Vandergheynst. Convolutional neural networks on graphs with fast localized spectral filtering. In *Advances in neural information processing systems*, pp. 3844–3852, 2016.

François Fouss, Kevin Francoisse, Luh Yen, Alain Pirotte, and Marco Saerens. An experimental investigation of kernels on graphs for collaborative recommendation and semisupervised classification. *Neural networks*, 31:53–72, 2012.

Justin Gilmer, Samuel S Schoenholz, Patrick F Riley, Oriol Vinyals, and George E Dahl. Neural message passing for quantum chemistry. *arXiv preprint arXiv:1704.01212*, 2017.

Will Hamilton, Zhitao Ying, and Jure Leskovec. Inductive representation learning on large graphs. In *Advances in neural information processing systems*, pp. 1024–1034, 2017.

Yoon Kim. Convolutional neural networks for sentence classification. *arXiv preprint arXiv:1408.5882*, 2014.

Diederik P Kingma and Jimmy Ba. Adam: A method for stochastic optimization. *arXiv preprint arXiv:1412.6980*, 2014.

Thomas N Kipf and Max Welling. Semi-supervised classification with graph convolutional networks. *arXiv preprint arXiv:1609.02907*, 2016.

Johannes Klicpera, Aleksandar Bojchevski, and Stephan Günnemann. Predict then propagate: Graph neural networks meet personalized pagerank. In *International Conference on Learning Representations*, 2019a.

Johannes Klicpera, Stefan Weißenberger, and Stephan Günnemann. Diffusion improves graph learning. In *Advances in Neural Information Processing Systems*, pp. 13354–13366, 2019b.

James R Lee, Shayan Oveis Gharan, and Luca Trevisan. Multiway spectral partitioning and higher-order cheeger inequalities. *Journal of the ACM (JACM)*, 61(6):1–30, 2014.

Qimai Li, Zhichao Han, and Xiao-Ming Wu. Deeper insights into graph convolutional networks for semi-supervised learning. In *Proceedings of the Thirty-Second AAAI Conference on Artificial Intelligence (AAAI-18)*, pp. 3538–3545. Association for the Advancement of Artificial Intelligence, 2018a.

Qimai Li, Xiao-Ming Wu, Han Liu, Xiaotong Zhang, and Zhichao Guan. Label efficient semi-supervised learning via graph filtering. In *Proceedings of the IEEE/CVF Conference on Computer Vision and Pattern Recognition (CVPR)*, June 2019.

Ruoyu Li, Sheng Wang, Feiyun Zhu, and Junzhou Huang. Adaptive graph convolutional neural networks. *arXiv preprint arXiv:1801.03226*, 2018b.

Naoki Masuda, Mason A Porter, and Renaud Lambiotte. Random walks and diffusion on networks. *Physics reports*, 716:1–58, 2017.

Lawrence Page, Sergey Brin, Rajeev Motwani, and Terry Winograd. The pagerank citation ranking: Bringing order to the web. Technical report, Stanford InfoLab, 1999.

S Pan, R Hu, G Long, J Jiang, L Yao, and C Zhang. Adversarially regularized graph autoencoder for graph embedding. In *IJCAI International Joint Conference on Artificial Intelligence*, 2018.

Bo Pang and Lillian Lee. Seeing stars: Exploiting class relationships for sentiment categorization with respect to rating scales. *arXiv preprint cs/0506075*, 2005.

Bryan Perozzi, Rami Al-Rfou, and Steven Skiena. Deepwalk: Online learning of social representations. In *Proceedings of the 20th ACM SIGKDD international conference on Knowledge discovery and data mining*, pp. 701–710, 2014.

Anand Rajaraman and Jeffrey David Ullman. *Mining of massive datasets*. Cambridge University Press, 2011.

Alexander J. Smola and Risi Kondor. Kernels and regularization on graphs, 2003.

Jian Tang, Meng Qu, Mingzhe Wang, Ming Zhang, Jun Yan, and Qiaozhu Mei. Line: Large-scale information network embedding. In *Proceedings of the 24th international conference on world wide web*, pp. 1067–1077, 2015.

Petar Veličković, Guillem Cucurull, Arantxa Casanova, Adriana Romero, Pietro Lio, and Yoshua Bengio. Graph attention networks. *arXiv preprint arXiv:1710.10903*, 2017.

Petar Velickovic, William Fedus, William L Hamilton, Pietro Lio, Yoshua Bengio, and R Devon Hjelm. Deep graph infomax. In *ICLR (Poster)*, 2019.

Felix Wu, Tianyi Zhang, Amauri Holanda de Souza Jr, Christopher Fifty, Tao Yu, and Kilian Q Weinberger. Simplifying graph convolutional networks. *arXiv preprint arXiv:1902.07153*, 2019.

Keyulu Xu, Weihua Hu, Jure Leskovec, and Stefanie Jegelka. How powerful are graph neural networks? In *International Conference on Learning Representations*, 2018a.

Keyulu Xu, Chengtao Li, Yonglong Tian, Tomohiro Sonobe, Ken-ichi Kawarabayashi, and Stefanie Jegelka. Representation learning on graphs with jumping knowledge networks. In *International Conference on Machine Learning*, pp. 5453–5462, 2018b.

Zhilin Yang, William Cohen, and Ruslan Salakhudinov. Revisiting semi-supervised learning with graph embeddings. In *International conference on machine learning*, pp. 40–48. PMLR, 2016.

Liang Yao, Chengsheng Mao, and Yuan Luo. Graph convolutional networks for text classification. In *Proceedings of the AAAI Conference on Artificial Intelligence*, volume 33, pp. 7370–7377, 2019.

Xiaotong Zhang, Han Liu, Qimai Li, and Xiao-Ming Wu. Attributed graph clustering via adaptive graph convolution. *arXiv preprint arXiv:1906.01210*, 2019.

A Supplementary Material

A.1 Node Clustering

For S^2GC and AGC, we set max iterations to 60. For other baselines, we follow the parameter settings in the original papers. In particular, for DeepWalk, the number of random walks is 10, the number of latent dimensions for each node is 128, and the path length of each random walk is 80. For DNGR, the autoencoder is of three layers with 512 neurons and 256 neurons in the hidden layers respectively. For GAE and VGAE, we construct encoders with a 32-neuron hidden layer and

Table 11: The statistics of datasets used for node classification and clustering.

Dataset	# Nodes	# Edges	class	feature	Train/Dev/Test Nodes
Cora	2, 708	5, 429	7	1433	140/500/1, 000
Citeseer	3, 327	4, 732	6	3703	120/500/1, 000
Pubmed	19, 717	44, 338	3	500	60/500/1, 000
Reddit	232, 965	11, 606, 919	41	602	152K/24K/55K
wiki	2405	17981	17	4973	

a 16-neuron embedding layer, and train the encoders for 200 iterations using the Adam optimizer with learning rate equal 0.01. For ARGE and ARVGE, we construct encoders with a 32-neuron hidden layer and a 16-neuron embedding layer. The discriminators are built by two hidden layers with 16 and 64 neurons respectively. On Cora, Citeseer and Wiki, we train the autoencoder-related models of ARGE and ARVGE for 200 iterations with the Adam optimizer, with the encoder and discriminator learning rates both set as 0.001; on Pubmed, we train them for 2000 iterations with the encoder learning rate 0.001 and the discriminator learning rate 0.008.

A.2 Text Classification

The 20NG dataset1 (bydate version) contains 18,846 documents evenly categorized into 20 different categories. In total, 11,314 documents are in the training set and 7,532 documents are in the test set.

The Ohsumed corpus2 is from the MEDLINE database, which is a bibliographic database of important medical literature maintained by the National Library of Medicine. In this work, we used the 13,929 unique cardiovascular diseases abstracts in the first 20,000 abstracts of the year 1991. Each document in the set has one or more associated categories from the 23 disease categories. As we focus on single-label text classification, the documents belonging to multiple categories are excluded so that 7,400 documents belonging to only one category remain. 3,357 documents are in the training set and 4,043 documents are in the test set.

R52 and R8 (all-terms version) are two subsets of the Reuters 21578 dataset. R8 has 8 categories, and was split to 5,485 training and 2,189 test documents. R52 has 52 categories, and was split to 6,532 training and 2,568 test documents.

MR is a movie review dataset for binary sentiment classification, in which each review only contains one sentence (Pang & Lee, 2005) The corpus has 5,331 positive and 5,331 negative reviews. We used the training/test split in (Tang et al., 2015).

A.3 Open Graph Benchmark: Node Property Prediction

A.3.1 Text Classification

Parameters. We follow the setting of Text GCN (Yao et al., 2019) that includes experiments on four widely used benchmark corpora such as 20-Newsgroups (20NG), Ohsumed, R52 and R8 of Reuters 21578. For Text GCN, SGC, and our approach, the embedding size of the first convolution layer is 200 and the window size is 20. We set the learning rate to 0.02, dropout rate to 0.5 and the decay rate to 0. The 10% of training set is randomly selected for validation. Following (Kipf & Welling, 2016), we trained our method and Text GCN for a maximum of 200 epochs using the Adam (Kingma & Ba, 2014) optimizer, and we stop training if the validation loss does not decrease for 10 consecutive epochs. The text graph was built according to steps detailed in the supplementary material.

To convert text classification into the node classification on graph, there are two relationships considered when forming graphs: (i) the relation between documents and words and (ii) the connection between words. For the first type of relations, we build edges among word nodes and document nodes based on the word occurrence in documents. The weight of the edge between a document node and a word node is the Term Frequency-Inverse Document Frequency (Rajaraman & Ullman,

Table 12: The statistics of datasets for text classification.

Dataset	# Docs	# Training	# Test	# Words	# Nodes	# Classes	Average Length
20NG	18,846	11,314	7,532	42,757	61,603	20	221.26
R8	7,674	5,485	2,189	7,688	15,362	8	65.72
R52	9,100	6,532	2,568	8,892	17,992	52	69.82
Ohsumed	7,400	3,357	4,043	14,157	21,557	23	135.82
MR	10,662	7,108	3,554	18,764	29,426	2	20.39

2011) (TF-IDF) of the word in the document applied to build the Docs-words graph. For the second type of relations, we build edges in graph among word co-occurrences across the whole corpus. To utilize the global word co-occurrence information, we use a fixed-size sliding window on all documents in the corpus to gather co-occurrence statistics. Point-wise Mutual Information (Church & Hanks, 1990) (PMI), a popular measure for word associations, is used to calculate weights between two word nodes according to the following definition:

$$\text{PMI}(i,j) = \log \frac{p(i,j)}{p(i)p(j)} \tag{14}$$

where $p(i,j) = \frac{W(i,j)}{W}$, $p(i) = \frac{W(i)}{W}$. $\#W(i)$ is the number of sliding windows in a corpus that contain word i, $\#W(i,j)$ is the number of sliding windows that contain both word i and word j, and $\#W$ is the total number of sliding windows in the corpus. A positive PMI value implies a high semantic correlation of words in a corpus, while a negative PMI value indicates little or no semantic correlation in the corpus. Therefore, we only add edges between word pairs with positive PMI values:

$$\mathbf{A} = \left[\begin{array}{c|c} \mathbf{W}_1 & \mathbf{W}_2 \\ \hline \mathbf{W}_2^\top & \mathbf{I} \end{array}\right]$$

or

$$A_{ij} = \begin{cases} \text{PMI}(i,j) & \text{if } i,j \text{ are words, PMI}(i,j) > 0, \\ \text{TF-IDF}_{ij} & \text{if } i \text{ is document, } j \text{ is word,} \\ 1 & \text{if } i = j, \\ 0 & \text{otherwise.} \end{cases} \tag{15}$$

A.4 Theoretical analysis

Below we show that we can reduce oversmoothing compared to SGC while incorporating larger receptive fields.

Our design contains a sum of consecutive diffusion matrices $\widetilde{\mathbf{T}}^k, k = 0, \cdots, K$. As k increases, so does the neighbourhood of each node visited in diffusion $\widetilde{\mathbf{T}}^k$ (analogy to random walks).

This means that:

Claim I. Our filter, by design, will give the highest weight to the closest neighborhood of a node as neighborhoods $\mathcal{N}$ of diffusion steps $k = 0, \cdots, K$ obey: $\mathcal{N}(\widetilde{\mathbf{T}}^0) \subseteq \mathcal{N}(\widetilde{\mathbf{T}}^1) \subseteq \cdots \subseteq \mathcal{N}(\widetilde{\mathbf{T}}^K) \subseteq \mathcal{N}(\widetilde{\mathbf{T}}^\infty)$. That is, smaller neighbourhoods belong to larger neighbourhoods too.

To see this clearer, for the q-dimensional Euclidean lattice graph with infinite number of nodes, after t steps of random walk, the estimate of absolute distance the walk moves from the source to its current position is given as:

$$r(t,q) = \sqrt{\frac{2t}{q}} \cdot \frac{\Gamma\left(\frac{q+1}{2}\right)}{\Gamma\left(q+1\right)}, \tag{16}$$

where $r(t,q)$ is the absolute distance walked from the source to the current point and $\Gamma(\cdot)$ is the Gamma function. Moreover, if the number of dimensions $q \to \infty$, we have $r(t,q) \leq \sqrt{t}$. It is clear then that the receptive field associated with the random walk (and thus diffusion at time t) obeys the

monotonically increasing radius r, that is $r(0) \leq r(1) \leq \cdots \leq r(K) \leq \cdots \leq r(\infty)$. To see that, simply plot $\sqrt{t}$ (and/or the more complicated expression).

This proves Claim I for the Euclidean lattice graph. That is, for consecutive diffusion steps $\widetilde{\mathbf{T}}^k, k = 0, \cdots, K$, our receptive field grows.

Moreover, note that our filter is realized as the sum of consecutive diffusion steps, that is $\frac{1}{t}\sum_{\tau=0}^{t} \text{diff}(s, \tau)$ where s is the source of walk. It is easy to see then that even if each walked distance was to contribute the energy proportional with $r(t)$ to the summation term, we have:

$$\lim_{t\to\infty} \frac{\frac{1}{t}\sum\limits_{t'=0}^{t} \sqrt{t'}}{\sqrt{t}} = 0, \tag{17}$$

where the enumerator is the model of the total energy when aggregating over receptive fields from size 0 to ∞ in S^2GC while the denominator is the total energy of SGC (filter is given by $\widetilde{\mathbf{T}}^K$, that is by $\text{diff}(s, t)$).

Claim II. The above proof shows that the above ratio of energies is 0 tells that the energy of infinite-dimensional receptive field (when $t \to \infty$) is not going to dominate the sum energy of our filter. Thus, according to this model S^2GC can incorporate larger receptive fields without overbearing contributions of smaller receptive fields compared to SGC as $t \to \infty$ on the Euclidean lattice graph.

However, in practice, we work with finite-dimensional non-Euclidean graphs. Obtaining the absolute distance $r(t)$ walked from the source is a difficult topic. Kindly see for instance Eq. 184 in Masuda et al. (2017).

For this reason, below we use a simple approximation. We use Theorem 1 (main paper) as the proxy for the walked radius. That is to say the error of convergence to the stationary distribution is indicative of the absolute distance walked from the source/node. Specifically, we have:

Recall Theorem 1. That is, let λ_2 denote second largest eigenvalue of transition matrix $\widetilde{\mathbf{T}} = \mathbf{D}^{-1}\mathbf{A}$, $\mathbf{p}(t)$ be the probability distribution vector and $\boldsymbol{\pi}$ the stationary distribution. If walk starts from the vertex i , $p_i(0) = 1$, then after t steps for every vertex:

$$|p_j(t) - \pi_j| \leq \sqrt{\frac{d_j}{d_i}}\lambda_2^t, \tag{18}$$

Then, the average walked distance r from node i over t steps in a graph with n nodes and connectivity given by the second largest eigenvalue λ_2, denoted by $r(i, t, n)$ is lower-bounded by $\bar{r}(i, t, n)$ as follows:

$$r(i, t, n) \approx \frac{1}{\frac{1}{n}\sum\limits_{j\neq i} |p_j(t) - \Pi_j|} \geq \bar{r}(i, t, n) = \frac{n}{\lambda_2^t \frac{\sum j\neq i \sqrt{d_j}}{\sqrt{d_i}}} = \frac{n\sqrt{d_i}}{\lambda_2^t(2|E| - d_i)}, \tag{19}$$

where n is the number of nodes, t is the number of diffusion steps (think $\widetilde{\mathbf{T}}^k$), d_i and d_j are degrees of nodes i and j, λ_2 being the second largest eigenvalue intuitively denotes the graph connectivity (large $\lambda_2 \leq 1$ indicates low connectivity while low λ_2 indicates high connectivity in graph), and $|E|$ is the total number of edges in the graph.

While the above approximations may be loose for very small/large t, the important property to note is that $r(i, 0, n) \leq r(i, 1, n) \leq \cdots \leq r(i, t, n)$ which indicates that our filter indeed realises the sum over increasingly larger receptive fields. As smaller receptive fields are a subset of larger receptive fields given node i, that is $\mathcal{N}(\widetilde{\mathbf{T}}^0) \subseteq \mathcal{N}(\widetilde{\mathbf{T}}^1) \subseteq \cdots \subseteq \mathcal{N}(\widetilde{\mathbf{T}}^K) \subseteq \mathcal{N}(\widetilde{\mathbf{T}}^\infty)$, this proves our Claim I.

To prove Claim II for general graphs, we have:

$$\lim_{t\to\infty} \frac{\frac{1}{t}\sum\limits_{t'=0}^{t} \bar{r}(i, t', n)}{\bar{r}(i, t, n)} = 0, \tag{20}$$

Similar findings are highlighted by carefully considering the meaning of so-called Cheeger constant introduced in Section A.5. More on spectral analysis of filters in GCNs can be found in the studies of Li et al. (2018a) and Li et al. (2018b).

A.5 GRAPH PARTITIONING

Below we introduce the definitions of expansion and k-way Cheeger constant.

Definition A.1. Expansion: For a node subset $S \subseteq V, \phi(S) = \frac{|\mathrm{E}(S)|}{\min\{\mathrm{vol}(S), \mathrm{vol}(V \setminus S)\}}$,

where $\mathrm{E}(\mathbf{S})$ is the set of edges with one node in $\mathbf{S}$ and $\mathrm{vol}(\mathbf{S})$ is the sum of degree of nodes in set S.

Definition A.2. The k-way Cheeger constant is given as: $\rho_G(k) = \min_{S_1, S_2, \cdots, S_k} \max\{\phi(S_i) : i = \{1, \cdots, k\}\}$ where the minimum is over all collections of k non-empty disjoint subsets $S_1, S_2, \cdots, S_k \subseteq V$.

According to the definitions, the expansion in Def. A.1 describes the effect of graph partitioning according to subset S while the k-way Cheeger constant reflects the effect of the graph partitioning into k parts–the smaller the value the better the partitioning is. Higher-order Cheeger's inequality (Bandeira et al., 2013; Lee et al., 2014) bridges the gap between the network spectral analysis and graph partitioning by controlling the bounds of k-way Cheeger constant:

$$\frac{\lambda_k}{2} \leq \rho_G(k) \leq \mathcal{O}\left(k^2\right) \sqrt{\lambda_k}, \tag{21}$$

where λ_k is the k-th eigenvalue of the normalized Laplacian matrix and $0 = \lambda_1 \leq \lambda_2 \leq \cdots \leq \lambda_n$. From inequality 21, we can conclude that small (large) eigenvalues control global clustering (local smoothing) effect of the graph partitioned into a few large parts (many small parts).